Land-cover change and environmental impact analysis in the Greater Mankato area of Minnesota using remote sensing and...

Article *in* International Journal of Remote Sensing · February 2008

DOI: 10.1080/01431160701294703

CITATIONS
69

READS
69

1 author:

Fei Yuan
Minnesota State University, Mankato
32 PUBLICATIONS **1,324** CITATIONS

SEE PROFILE

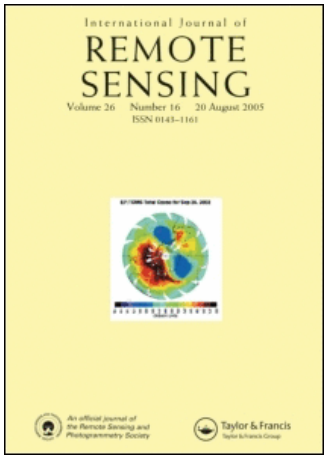

International Journal of Remote Sensing
Publication details, including instructions for authors and subscription information:
http://www.informaworld.com/smpp/title~content=t713722504

Land-cover change and environmental impact analysis in the Greater Mankato area of Minnesota using remote sensing and GIS modelling

F. Yuan [a]
[a] Department of Geography, Minnesota State University - Mankato, Mankato, MN 56001

Online Publication Date: 01 February 2008
To cite this Article: Yuan, F. (2008) 'Land-cover change and environmental impact analysis in the Greater Mankato area of Minnesota using remote sensing and GIS modelling', International Journal of Remote Sensing, 29:4, 1169 - 1184
To link to this article: DOI: 10.1080/01431160701294703
URL: http://dx.doi.org/10.1080/01431160701294703

International Journal of Remote Sensing
Vol. 29, No. 4, 20 February 2008, 1169–1184

Land-cover change and environmental impact analysis in the Greater Mankato area of Minnesota using remote sensing and GIS modelling

F. YUAN*
Department of Geography, Minnesota State University—Mankato, Mankato, MN 56001, USA

(*Received 31 December 2006; in final form 16 February 2007*)

Land use and land-cover (LULC) data provide essential information for environmental management and planning. This research evaluates the land-cover change dynamics and their effects for the Greater Mankato Area of Minnesota using image classification and Geographic Information Systems (GIS) modelling in high-resolution aerial photography and QuickBird imagery. Results show that from 1971 to 2003, urban impervious surfaces increased from 18.3% to 32.6%, while cropland and grassland decreased from 54.2% to 39.1%. The dramatic urbanization caused evident environmental impacts in terms of runoff and water quality, whereas the annual air pollution removal rate and carbon storage/sequestration remained consistent since urban forests were steady over the 32-year span. The results also indicate that highly accurate land-cover features can be extracted effectively from high-resolution imagery by incorporating both spectral and spatial information, applying an image-fusion technique, and utilizing the hierarchical machine-learning Feature Analyst classifier. This research fills the high-resolution LULC data gap for the Greater Mankato Area. The findings of the study also provide valuable inputs for local decision-makers and urban planners.

1. Introduction

Land-use and land-cover changes (LULCC) have great effects for the environmental and socio-economic sustainability of communities. When one type of use replaces another, the effects tend to be superimposed and cumulative. During the process of urbanization, when rural areas are converted to urban land uses, hydrological circle and rates of soil erosion will change accordingly (Tong and Chen 2002). Meanwhile, when agricultural land is decreasing, the dependence on the use of fertilizers and pesticides to increase the productivity is rising. As a consequence, unused nutrients, mainly nitrogen and phosphorus, near the soil surface could be transported by surface runoff to water bodies, thereby degrading water quality by causing eutrophication (Tilman *et al.* 2001). The amount of urban impervious surfaces has emerged as an important indicator of environmental quality (Arnold and Gibbons 1996). It influences the non-point source pollution and water quality by directly affecting the amount of runoff to water bodies (Dougherty *et al.* 2004). In addition, because of the heat-storage capacities of urban impervious surfaces, as well as waste heat from transportation and industry, the temperatures are usually higher

*Email: fei.yuan@mnsu.edu

International Journal of Remote Sensing
ISSN 0143-1161 print/ISSN 1366-5901 online
http://www.tandf.co.uk/journals
DOI: 10.1080/01431160701294703

in the city (Oke 1976, Eliasson 1992, Weng 2001a). As a result, the higher temperatures in urban areas increase air conditioning demands and affect local climate by affecting the energy balance and thus modifying precipitation patterns (Carlson and Arthur 2000). Moreover, urbanization leads to habitat fragmentation and irreversible resource loss (Collinge 1996, Nikolakaki 2004). The expanding city is a remarkable producer of wastes and causes large problems of environmental pollution as well.

An integrated remote sensing and Geographical Information Systems (GIS) modelling method has become a trend for environmental assessment and management for its capabilities of managing and manipulating large amounts spatial data to satisfy planner and policymaker's growing needs of accurate LULCC information. For instance, Weng (2001a) evaluated the impacts of urban expansion on surface temperature and surface runoff (Weng 2001b) in the Zhujiang Delta of South China using the integrated method. Findings from these studies indicated that urban development had raised the surface radiant temperature by 13 K in the urbanized area and had increased the annual runoff depth by 8.1 mm during the 1989–1997 periods. Tong and Chen (2002) modelled the relationship between land use and surface water quality in the State of Ohio. Their study revealed that there was a significant relationship between land use and in-stream water quality, especially for nitrogen, phosphorus, and faecal coliforms. In particular, agricultural and impervious urban lands produced a much higher level of nitrogen and phosphorus than other land surfaces. Arthur *et al.* (2003) performed satellite and ground-based microclimate and hydrologic analyses coupled with a regional urban growth model in south-eastern Pennsylvania. Gillies *et al.* (2003) derived the impervious surface area (ISA) from 1979 to 1997 for the Line Creek Watershed located to the south of the city of Atlanta, GA, and reported evident mussel habitat degradation and loss of species in areas where ISA expansion was observed. Milesi *et al.* (2003) reported that an increase in urban development for the south-eastern United States of 1.9% during the 1992–2000 period reduced the annual net primary production (NPP) of the south-eastern United States by 0.4%. Claggett *et al.* (2004) assessed development pressure in the Baltimore–Washington, DC region using a cellular automata model and a supply/demand allocation model. Carlson (2004) analysed and predicted surface runoff by simple runoff calculations and an urban growth model for Spring Creek Watershed in Central Pennsylvania. Weng and Yang (2006) analysed the relationship between the local air pollution pattern and urban land use for Guangzhou in China. They reported that the spatial patterns of air pollutants were positively correlated with urban built-up density and land surface temperature. Ode and Fry (2006) assessed urban pressure on woodland for the Malmő-Lund region in Sweden using a GIS-based model.

The findings of earlier studies on environmental impacts of LULCC have been conducted mainly at regional scales in 30-m Landsat or coarser spatial resolution imagery, which offer possibilities for monitoring LULCC and their effects in a synoptic view. However, for local land use and urban planning purposes, the 30-m resolution is not enough. According to Antrop (2004), only sub-5-m resolution may provide satisfactory results in a highly heterogeneous urban environment. The recent availability of high-resolution satellite remote-sensing images coupling with historical aerial photography offers an improved opportunity to monitor environment at local scales. Moreover, due to the increasing sizes of datasets obtained by modern remote sensing, accurate LULC extraction in a highly automated fashion

and environmental assessment using the extracted high-resolution LULC data as inputs is increasingly becoming a necessity.

This study aims to analyse land-cover changes and their environmental effects for the Greater Mankato Area in south central Minnesota from 1971 to 2003 by (1) extracting land-cover information from sub-1-m aerial photography and 2.4-m QuickBird satellite imagery using an innovative machine-learning automatic feature analysis; (2) exploring change statistics and patterns by post-classification comparison; and (3) assessing and modelling the major environmental (air quality, carbon storage and sequestration, water runoff and water quality) and economic impacts in relation to land-cover changes, especially urban forest and impervious surface changes.

This research fills the high-resolution LULC data gap for the Greater Mankato Area. In this area, reliable LULC information derived from remote-sensing images is limited, although historically there have been several sources of statistical inventory data available, for example the US Department of Agriculture's Agricultural Census and the Natural Resources Conservation Service (NRCS)'s Natural Resource Inventory (NRI). Both of the inventories are collected every five years. Nevertheless, there is no means to tie their statistics to specific geographic locations, and the NRI always lags in its reporting for four–five years (Sawaya *et al.* 2001). In addition, the National Land Cover Data (NLCD) of 1992 and 2001 are based on 30-m Landsat data, which are not suitable for local scale city-level studies (Ridd 1995, Foody 1999, Antrop 2004).

Moreover, the study benefits both the scientific community and local decision-makers by addressing the following key issues. How can one extract accurate land use and land-cover information effectively from historical aerial photography and recent high-resolution satellite images? What are the land-cover change patterns, rate, and characteristics over the last three decades in the Greater Mankato Area? How can urban trees and impervious surface affect air quality, carbon storage/sequestration, surface runoff, and water quality? What are the associated economic values of urban environmental changes?

2. Method

2.1 *Study area*

The Greater Mankato Area includes two cities, Mankato and North Mankato, located along the Minnesota River in south central Minnesota (figure 1). According to the United States Census Bureau, the city of Mankato covers an area of 39.8 km^2 with a total population of 32 427 in 2000. Its sister city North Mankato has a total area of 12.4 km^2 and approximately 11 798 people in the same census. As a regional centre for employment, shopping, educational enrichment, and social and recreational events, land use and land cover in this area have undergone remarkable changes over the last several decades. For example, according to a recent study (Bauer *et al.* 2005), the total impervious surface area of the Greater Mankato area increased by 50% from 1990 to 2000. As cities grow, they expand over agriculture, wetland, grassland, and forest, thereby changing the physical shape of the landscape and the functioning state of the ecosystem. Consequently, accurate land-use and land-cover change information and its cause-and-effect analysis are critical to provide a suitable direction for policy- and decision-makers in this area.

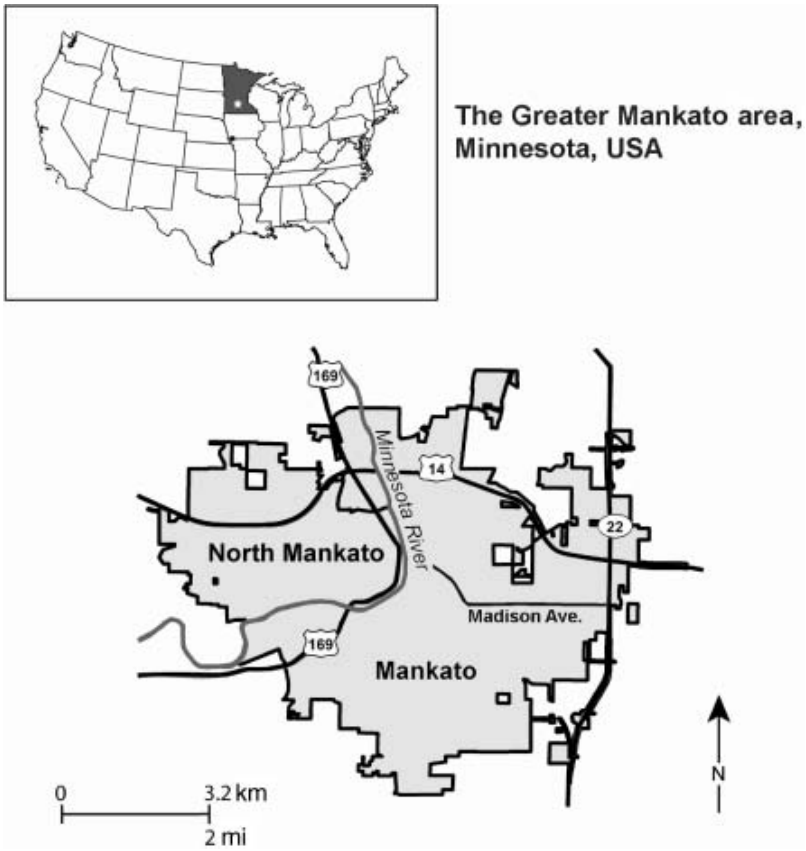

Figure 1. Greater Mankato area of Minnesota, USA.

2.2 *Data preprocessing*

Remote-sensing data of multiresources including high-resolution air photographs, National Agricultural Imagery Programme (NAIP) colour digital orthophoto, and QuickBird satellite imagery covering the study area from 1971 to 2003 were acquired. Specifically, the 9-inch 0.6-m black and white (B&W) air photographs of 1971 were obtained from the historical map collection of the Minnesota State University Library. The 2003 1-m NAIP digital orthophoto mosaic of Blue Earth County was provided by the Land Management Information Centre (LMIC) of Minnesota. The QuickBird imagery on 6 October 2003 was acquired from the Standard Imagery products of Digital Globe. The QuickBird data are recorded in unsigned 16 bits and include four multispectral bands at 2.4-m resolution and one panchromatic band at 0.6-m resolution. The data were radiometrically and geometrically corrected but were not fully orthorectified, although a coarse Digital Elevation Model (DEM) was used to normalize the effects of topographic relief (Eurimage 2006). Moreover, a 10-m DEM to be used as one of the input layers for the GIS modelling was obtained from the US Geological Survey (USGS).

The 1971 photographs were scanned at 600 dpi and 16 bits-per-pixel colour and imported to ERDAS IMAGINE™ image files. All images were first georectified to UTM zone 15, GRS1980, NAD83 using 2000 Street Map as the reference. No orthorectification was performed due to the limitation of missing camera parameters for these historical aerial photos. Next, the georectified images were mosaicked. Since the 1971 images were acquired on different dates with varying atmospheric

and illumination conditions, a histogram matching function was utilized in the mosaic. The 2003 QuickBird data were reprojected from the original WGS projection to UTM and georectified again to match the 2003 NAIP colour digital orthophoto. Finally, all three different datasets were clipped within the limits of our study area using the Municipal Boundary shapefile obtained from the Data Deli website of Minnesota Department of Natural Resource (DNR) (http://deli.dnr.state.mn.us/).

2.3 *Extraction of land cover and change information using Feature Analyst*

While all the datasets have a high spatial resolution, their spectral and radiometric resolutions vary. Comparatively, the 1971 black and white photography contains the lowest amount of spectral and radiometric information, while the opposite is true for the QuickBird image. To guarantee accurate and effective land-cover extraction and change analysis from these data, four land-cover classes—impervious surface, forest, cropland/grass, and water—were defined in our classification scheme. In particular, since it is very difficult to differentiate cropland and grassland in the B&W imagery, the two land covers were defined as one single mixture class. However, extracting these four different land covers from the 1971 data automatically is still challenging because of the low spectral variation and the complex landscapes in the photo. For example, certain classes such as bare fields and impervious surfaces, and some crop fields and forests have very similar spectral responses, which make it difficult to distinguish them from each other. To address this problem, a 3×3 second-order (variance) texture analysis was applied to the 1971 aerial photography. Variance is a measure of heterogeneity which increases when the grey level values differ from their mean (equation (1)).

$$\text{Variance} = \frac{\sum \left(x_{ij} - \frac{\sum x_{ij}}{n} \right)^2}{n-1}, \tag{1}$$

where x_{ij} is the digital number (DN) value of pixel (i, j), and n is the number of pixels in the 3×3 window (Leica Geosystems 2005).

The resulting texture image from the analysis was then stacked with the original 1971 aerial photo as an additional layer for land-cover extraction. It is known that proper texture measurements are helpful for segmenting and classifying an image (Gong and Howarth 1990, Baraldi and Parmiggiani 1995, Ryherd and Woodcock 1996, Zhang 1999, Herold *et al.* 2003). In this study, since forest and urban impervious surface demonstrate much more heterogeneous textures from the homogenous patterns of crop field, the texture image greatly increased the discrimination of land covers. It also helped to minimize classification errors caused by varying atmospheric and illumination conditions of the mosaiced image.

In the case of the 2003 image classification, both the summer NAIP colour air photography and the early autumn QuickBird Image were utilized. In particular, the QuickBird data set has four multispectral bands with a spatial resolution of 2.4 m. It also has a panchromatic band with 0.6-m resolution. Using the Principle Component Merge technique of ERDAS IMAGINE™, these multispectral and panchromatic bands were fused to provide a four-band image with 0.6-m resolution, which was then resampled and stacked with the three-band 1-m colour NAIP to obtain a seven-band image. One purpose of image fusion is to integrate different data to obtain more information than can be derived from each of the single sensor

data alone (Pohl and Van Genderen 1998), thereby producing a higher classification accuracy than can be obtained from a single date image (Coppin and Bauer 1994, Wolter *et al.* 1995, Reese *et al.* 2002, Yuan *et al.* 2005) by reducing the misclassified class due to similar spectral responses between harvested cropland and an urban impervious area.

Another reason to use both 2003 NAIP and QuickBird images is to minimize shadow problems in high-resolution images. Shadows can cause unclear results and are difficult to address because of the complicated fact that shadows include not only tree shadows but also building shadows that may occur in both pervious and impervious areas (Yuan and Bauer 2006). Since the 2003 October QuickBird image was acquired with a relatively low Sun elevation angle of 38.5°, building and tree shadows were relatively severe for this image. On the other hand, the 2003 summer colour NAIP digital air photograph demonstrated fewer building and tree shadows. These shadows are in different directions from those of QuickBird due to the dissimilar Sun-target-sensor geometry of NAIP. As a result, many shadows in the QuickBird imagery are not shadowed in the NAIP data and vice versa. Therefore, the stacked seven-band data were able to resolve the shadow problem successfully.

After training polygons with random distribution were digitized as separate shapefiles for each land-cover classes for both years, software designed particularly for classifying high-resolution data, Virtual Learning System's (VLS) Feature Analyst™, was used for the classification. It is known that standard per-pixel classifiers using pure spectral information are ineffective at extracting information from these new data sources (Herold *et al.* 2003, Thomas *et al.* 2003). Feature Analyst™ uses spatial context as well as spectral information. It also includes a contextual classifier that can be adjusted based on the feature to be extracted. Compared with a traditional land-cover classifier, Feature Analyst has two major advantages. First, it makes use of a foveal representation with a learning algorithm that gives a region of the image with a high spatial resolution at the centre and a lower resolution away from the centre. Thus, it provides contextual spatial information to the learning algorithm while greatly reducing the amount of data given to the learner. Second, Feature Analyst addresses image clutter with a hierarchical approach that allows the Classifier not only to learn from the user input and return like objects but also to improve classification results by mitigating clutter and retrieving missed features, which is also the major advantage of Feature Analyst™ compared with other object-oriented classifiers such as eCognition™ (Visual Learning Systems 2005).

Specifically, the first step of the hierarchical learning method is to create a training set of features using drawing tools. Next, the Feature Analyst Learner relies on several information inputs to determine whether or not image pixels represent the target feature that is identified in the training set. The information inputs include: 'input bands', which provide spectral data; 'input representations', which provide spatial data, and 'learning algorithms', which provide the mathematical calculations that tie it all together. Once the initial results are acquired, Feature Analyst™ then allows the user to define examples of correct, incorrect, and missed areas, which are then used as inputs to refine the classification map. Furthermore, the refinement process can be repeated as many times as necessary until the best results are achieved (Visual Learning Systems 2005). Using Feature Analyst™, each of the four land covers was extracted as a separate vector layer and then combined and converted to

1-m raster images for both years. Next, a 3×3 majority filter was applied to remove isolated pixels on the classification maps.

Finally, a stratified systematic random sampling was utilized to select 300 test samples for each year. Each sample has the uniform size of 1 pixel. The corresponding land covers for the test samples were derived and recorded by visually interpreting the 1971 air photograph and 2003 stacked image. Confusion matrices as simple cross-tabulations of the mapped class label against that observed in the reference data were utilized to assess the accuracy of classification maps. Overall accuracy, user's and producer's accuracies, and the Kappa statistic were then derived from the confusion matrix.

2.4 *Environmental impact assessment using GIS modelling*

The environmental and economic impacts from land-use change, especially urban forest and impervious surfaces changes, were assessed using CITYgreen™, which works as an extension in ArcGIS™ Desktop. CITYgreen™ is a comprehensive and user-friendly tool that can be used to calculate the environmental benefits provided by urban trees and to model the impacts of various development and planning scenarios. It has four major functions of analysing air quality, carbon storage and sequestration, storm water runoff, and water-quality changes (American Forests 2004).

Specifically, it calculates the air-pollution removal value using the Urban Forest Effects (UFORE) Model, which was developed to quantify the urban forest structure and functions based on standard inputs of field, meteorological, and pollution data. The amounts of five air pollutants—ozone (O_3), sulphur dioxide (SO_2), nitrogen dioxide (NO_2), carbon monoxide (CO), and particulate matter smaller than 10 μm (PM10)—that can be removed by urban forest were calculated. The air-quality dataset used in this model was provided by the US Forest Service based on its research across the US. Further, the total carbon storage (the amount of carbon stored in the biomass of the trees on the study site) and annual carbon sequestration (the amount of additional carbon that is stored each year as the trees grow) by urban trees were then reported.

Based on the percentage of urban forest and other land covers and various site characteristics such as local rainfall patterns, soil type, and slope, five relevant numbers were calculated: (1) Curve Number (CN) which is a composite number that describes how much of the rainfall that falls on a site will run off and how quickly that will happen; (2) CN if the trees were replaced by impervious surfaces; (3) the volume of additional water to be managed if the trees were removed from the site; (4) the total storm water savings (the additional cost of managing your site's storm water without trees); and (5) the annual storm water values over 20 years at 6% interest (American Forests 2004).

In particular, CITYgreen™ uses the urban hydrology for small watersheds model, also referred to as Technical Release 55 (TR-55) storm water model that was developed by the NRCS to calculate CN (USDA 1986). In TR-55, the CN calculation method originated from USDA (1985). Specifically, it determines CN based on land cover and soil conditions, which the model represents as the hydrological soil group, cover type, and hydrologic condition (USDA 1985). A hydrological soil group code 'A', ' B', 'C', or 'D' is used as a measure of infiltration capacity of water in soils in the model. Soil type 'A' is very pervious with the highest rate of infiltration, but the opposite is true for soil type 'D'. Soil types 'B' and 'C' represent for groups that are less pervious and less impervious, respectively (USDA

1985, American Forests 2004). The hydrological soil group is an attribute of the soil mapping unit of STATSGO soil data. North Mankato has purely 'D' hydrological soil, though 'B' is dominant over Mankato area (USDA 1995). In CITYgreen™, CN for each pixel is based on the standard lookup tables that were provided in USDA (1985, 1986), whose value is sensitive to both hydrological soil type and land-cover type. In general, the value of CN increases steadily when the hydrological soil type changes from 'A' to 'D'. Also, the forest land cover has the lowest CN, whereas the urban impervious area has the highest value. The mean CN value of each land cover was calculated and then weighted to obtain a composite value for the entire site using equation (2) (American Forests 2004).

$$\mathrm{CN}_{\mathrm{Weighted}} = \frac{\sum \mathrm{PCT}_i \mathrm{CN}_i}{\sum \mathrm{PCT}_i}, \tag{2}$$

where PCT_i is the percent land-cover area, and CN_i is the average curve number for the land cover.

The resulting CN ranges from 30 to 100. The higher the CN value, the more runoff will occur, as shown in equation (3) (USDA 1985, 1986):

$$Q = \frac{\left(P - 0.2\left(\frac{1000}{\mathrm{CN}} - 10\right)\right)^2}{\left(P + 0.8\left(\frac{1000}{\mathrm{CN}} - 10\right)\right)}, \tag{3}$$

where Q is the runoff, and P is the average rainfall for a 24 h period.

Next, the relationship between the amount of pollutants present in the nearby water bodies and the composition of land cover was also modelled using values from the US Environmental Protection Agency (EPA) and Purdue University's Long-Term Hydrological Impact Analysis (L-THIA), which is a spreadsheet model coupling CN to quantify the percent change of specific water pollutants during a storm event. This model estimates the changes in concentrations of nitrogen, phosphorus, suspended solids, zinc, lead, copper, cadmium, chromium, chemical oxygen demand (COD), and biological oxygen demand (BOD) in runoff during a 24-h storm event (American Forests 2004). The rain value of 70 mm for this study is based on NRCS estimates of rainfall distributions for different regions of the US. In addition, the slope map utilized in this model was derived from the 10-m DEM data obtained from USGS. The average percentage slope of the Greater Mankato Area is 2.9.

3. Results

3.1 *Accuracies of land-cover classifications*

Error matrices were used to assess the accuracies of classifications and are summarized in table 1. The overall accuracies are greater than 92% for both years, while the Kappa statistics are 0.87 and 0.9, respectively, for 1971 and 2003. In comparison, the 2003 classification has a slightly higher accuracy with all User's and Producer's accuracies of individual classes over 90%, which is reasonable, since the fused colour NAIP and QuickBird image contains much more spectral information than the B&W aerial photography of 1971. These accurate assessment results indicate that reliable land-cover features can be extracted effectively from high-resolution imagery with the help of various digital image processing techniques such

Table 1. Error matrices for 1971 and 2003 classifications.

	Reference data				
	Impervious	Forest	Cropland/grass	Water	User's accuracy (%)
1971 classification					
Impervious	48	2	4	0	88.9
Forest	0	63	12	1	82.9
Rural	3	1	156	0	97.5
Water	0	0	0	10	100.0
Producer's accuracy	94.1%	95.5%	90.7%	90.9%	
Overall classification accuracy=92.3%			Overall kappa statistics=0.874		
2003 classification					
Impervious	89	0	4	1	94.7
Forest	0	64	5	0	92.8
Rural	3	7	115	0	92.0
Water	0	0	0	12	100.0
Producer's accuracy	96.7%	90.1%	92.7%	92.3%	
Overall classification accuracy=93.3%			Overall kappa statistics=0.901		

as texture analysis, image fusion, and the hierarchical machine-learning Feature Analyst classifier.

3.2 *Land-cover maps, statistics, and change characteristics*

Land-cover classification maps for both years are displayed in figure 2, which demonstrates that the occurrence of striking suburban expansions had occurred just outside the central cities in this region, from 1971 to 2003. More specifically, while forested and water areas are relatively stable, considerable urban growth and agriculture loss can be identified by comparing the 1971 and 2003 maps. The largest cluster of urban growth at the expense of the vast expanse of cropland is located in the north-eastern region along Madison Avenue, which runs east–west from downtown Mankato. This area is the current business and commercial centre of Mankato, where highway 22 located in a north–south direction intersects with highway 14 running in an east–west direction. Dramatic rural-to-urban conversions in the north, north-west, and south areas are also apparent in the post-classification change-detection map (figure 3).

Besides the major change of cropland to urban development, other types of conversions including forest to urban, forest to cropland/grassland, and vice versa can also be identified in figure 3. In particular, the cropland/grassland to forest change had occurred primarily along forest edges, whereas the opposite conversion had occurred mainly along major roads, especially highway 14. The individual class area and change statistics for both years are summarized in table 2, which shows that the urban impervious area increased by 83.2%, from 867 ha in 1971 to 1588 ha in 2003. Conversely, cropland and grassland decreased severely from 2638 ha to 1904 ha during the same 32-year span, implying that farm-based populations had been replaced significantly due to urbanization.

In terms of population growth, according to Adams *et al.* (2003), the Greater Mankato area experienced moderate population growth from 1970 to 2000. Specifically, Mankato's population of 30 895 in 1970 first dropped in the following decade but then increased to 32 427 by 2000, whereas the North Mankato

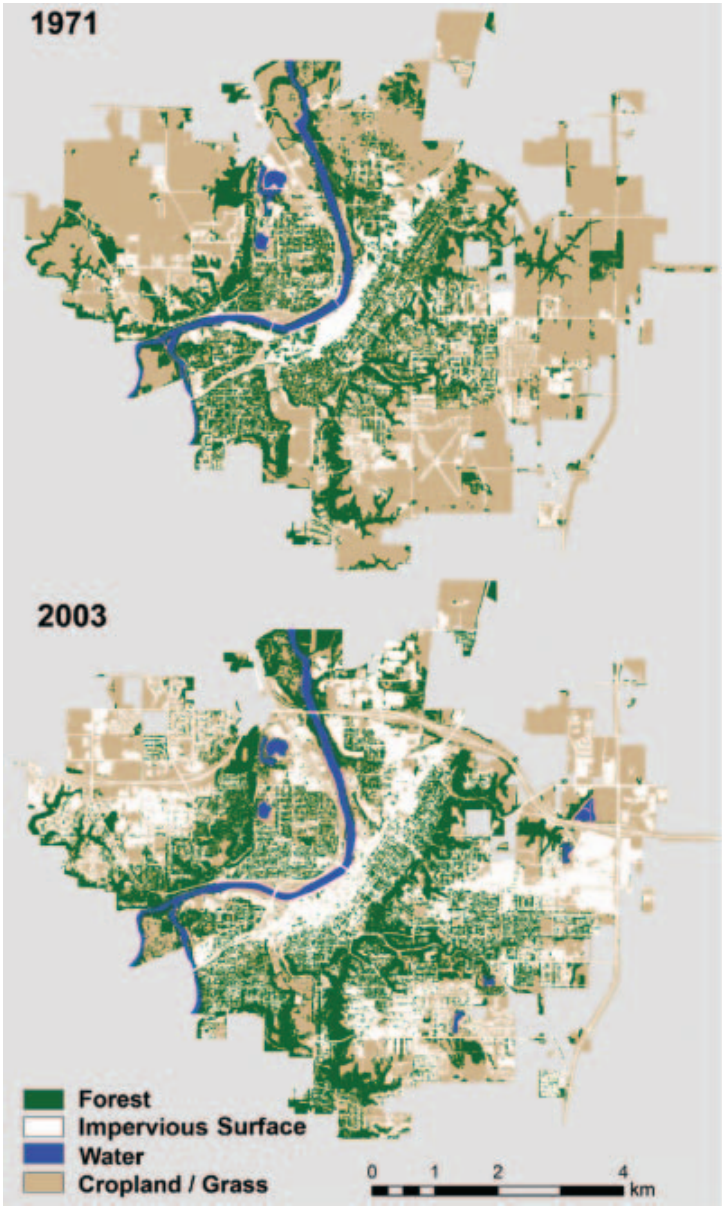

Figure 2. Land-cover classifications for 1971 and 2003.

population gained steadily each decade from 7347 in 1970 to 11 798 in 2000, which gives an annual population growth rate of approximately 0.5% for the whole area. Comparatively, the annual urban expansion rate of 2.6% for the same period is more than five times the rate of population increase. This further quantifies the dramatic degree of urban sprawl (rapid expansion of low-density suburbs into formerly rural areas) in this region. Sutton (2003) indicated that urban sprawl is occurring within urban boundaries where the population density is lower than the mean for an urban centre of a particular size. Therefore, urban sprawl implies that the land is less efficiently utilized than for the average.

3.3 *Environmental impacts from urban land-cover changes*

Urban trees perform a vital air-cleaning service by absorbing and filtering out air pollutants as well as removing carbon dioxide from the air through their leaves and

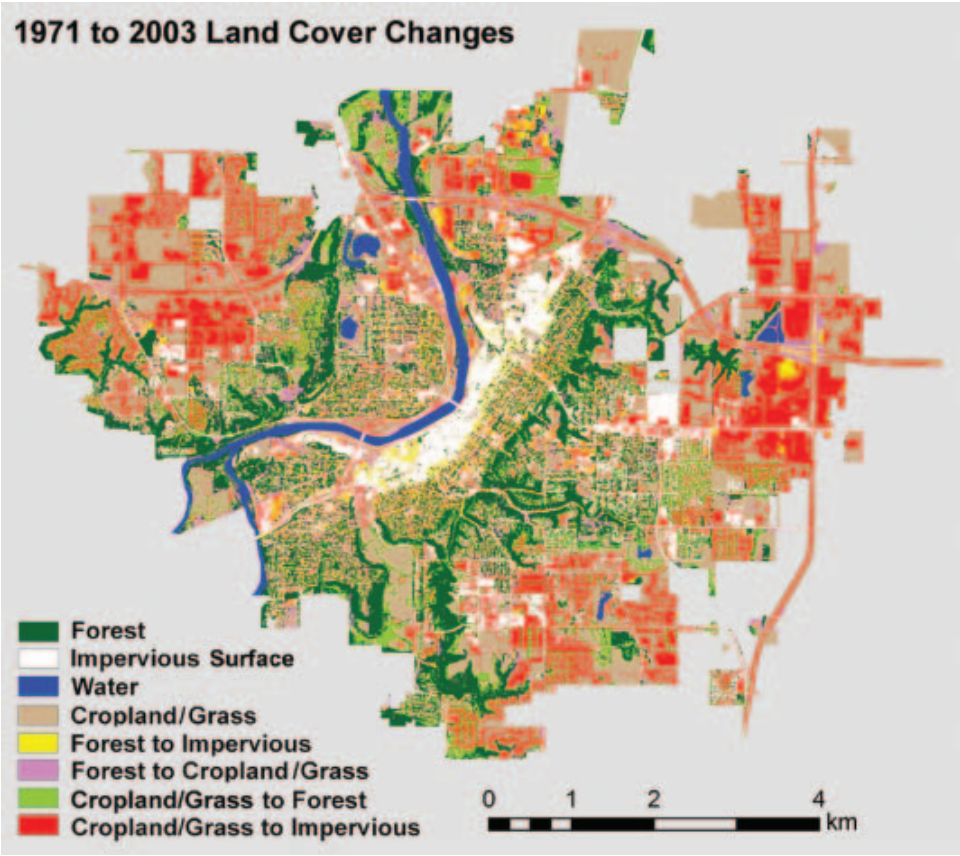

Figure 3. Land-cover change for 1971–2003.

storing carbon in their biomass. In CITYgreen™, linear relationships between the total volume of urban forest and the air-pollution removal rate and between the total volume of urban forest and carbon storage capacity are assumed. Table 3 presents the annual air-pollution removal rate of trees and the dollar values of the pollutants for this study site. Since the urban tree cover was very steady over the 32-year span, these two statistics are approximately equal to 77 000 kg and $450 000 per year for both 1971 and 2003, among which 57.14% is O_3, 27.65% is NO_2, and 13.54% is PM10. The estimated carbon storage capacity was about 130 000 tons, and the carbon sequestration rate of trees was about 1016 tonnes per year for both years.

In addition to urban trees, the storm-water runoff volume is determined by various factors of land-cover composite, soil type, and precipitation in addition to trees. For an average 70-mm 24-h storm for the Greater Mankato area, the corresponding values for storm water control are displayed in table 4. The CN

Table 2. Land-cover classification statistics for 1971 and 2003.

	1971		2003		Change	
Land-cover class	(ha)	(%)	(ha)	(%)	(ha)	(%)
Impervious surface	867	18.3	1588	32.6	721	83.2
Forest	1229	25.3	1250	25.7	21	1.7
Cropland	2638	54.2	1904	39.1	−734	−27.8
Water	108	2.2	123	2.5	15	13.9

Table 3. Annual air-pollution removal rate of trees and dollar values of pollutants in the Greater Mankato Area.

	1971		2003	
Air pollutant	Kilograms removed per year	Dollar value ($)	Kilograms removed per year	Dollar value ($)
CO	3675	3459	3738	3517
O_3	37 979	257 278	38 623	262 639
NO_2	18 377	124 489	18 688	126 599
PM	13 476	60 951	13 705	61 984
SO_2	2450	4055	2492	4123
Totals	75 958	450 231	77 245	457 863

numbers reflect the fact that existing land cover and soil conditions increased from 1971's 83 to 2003's 86. By inserting the two CN numbers into equation (3) separately, a 5.14-mm increase of surface runoff from 1971 to 2003 can be derived. Since the urban forested area was relatively consistent over the 32-year span, the rise in the volume of storm water runoff was mainly caused by the increased amount of urban impervious surface areas that occurred during the same time period.

Nevertheless, in a different scenario of 'assuming all the trees were removed' from the study site, we can see the important role that trees may play in decreasing total storm water volume and detention cost as well. For example, according to table 4, if all the trees were removed, the CN numbers would increase evidently from original 83 to 88 for 1971, and 86 to 91 for 2003. Consequently, the 'volume of additional water to be managed' if the trees were removed from the site for both years can also be calculated. The total storm-water savings number was then calculated by multiplying the volume of additional water by the construction cost. For this study site, the construction cost (fees of building a storm-water management facility to control the additional water) was assumed to be $70.6 per cubic metre by the model. Based on financing the total value at 6% interest over 20 years, the costs of yearly payments on a storm water facility were $2 660 963 and $2 959 604, respectively, for 1971 and 2003 if the trees in the study site were removed. In addition, figure 4 demonstrates the modelling results of percentage change in the amount of various pollutants in nearby bodies if all the trees of 2003 were removed from the site and replaced with impervious surface. Except for zinc and lead, all the other pollutants

Table 4. Effects of land-cover changes on storm-water runoff in the Greater Mankato Area.

Effects of land-cover changes on storm-water runoff	1971	2003
2-year, 24-h rainfall (mm)	70	70
CN reflecting existing conditions	83	86
CN if trees are replacement by impervious	88	91
Additional storm water storage volume needed (m^3)	432 117	480 613
Construction cost per m^3 ($)	$70.6	$70.6
Total storm-water savings ($)	$30 521 034	$33 946 421
Annual costs based on payments over 20 years at 6% Interest ($ per year)	$2 660 963	$2 959 604

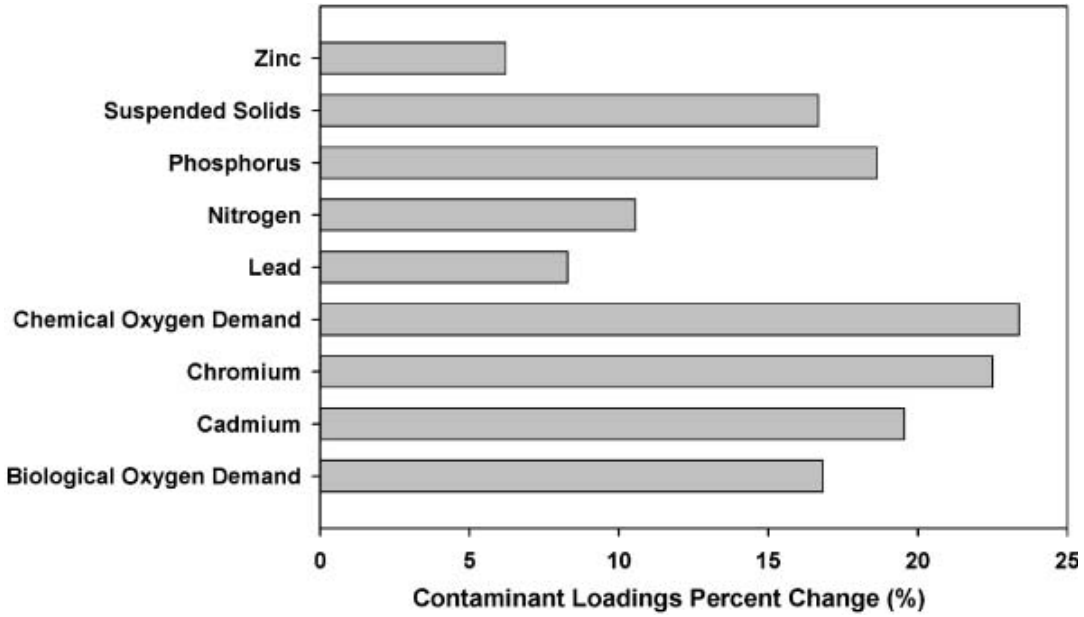

Figure 4. Change in concentration of pollutants in runoff during a typical storm event if the urban trees are removed in 2003 in the Greater Mankato Area.

have double-digit percentage increases, reflecting severe decreases in water quality with the increase of impervious surface.

4. Discussion and conclusions

This study evaluated general land-use patterns, major development trends, and environmental impacts of land-use change in the Greater Mankato area over the last three decades using an integrated method of remote sensing and GIS modelling. Dramatic urban expansion was found with moderate population growth. In particular, urban developed areas within the municipal boundary almost doubled from 18.3% in 1971 to 32.6% in 2003. Despite the rapid urban sprawl, the annual air-pollution removal rate and carbon storage/sequestration remained consistent due to the slightly increasing urban forest in this site over the 32-year span. However, urban sprawl had caused an evident increase (5.14 mm) in surface runoff. Impervious surface area and urban tree coverage were also positively associated with contaminant loadings in water bodies. These findings are in conformity with many studies that show a close relationship between urban impervious surface area and watershed viability (Schueler 1994, Carlson 2004). Nevertheless, this study is based on data within the urban municipal boundary, and it is not clear if the surface runoff and water quality results cited in this paper would be comparable if the assessment were performed in a watershed level instead of a municipal boundary. In addition, the carbon storage/sequestration estimation based only on urban tree coverage is not ideal, since tree age, type, and volume all affect the final carbon storage value.

The study also demonstrated that high-resolution satellite data coupled with historical aerial photography have excellent potential for extending environmental management and land-use planning to a local scale. Highly accurate land cover features can be extracted from high-resolution images of complex landscapes using various digital-image processing techniques. For historical B&W aerial photography

with a low spectral variation, the texture component is crucial, and the hierarchical learning approach provided by VLS's Feature Analyst is very useful. In addition, the shadow problem in high-resolution multi-spectral imagery can be resolved by image fusion. In this study, the summer NAIP colour air photo and the autumn QuickBird satellite image were fused by resolution merging. Since the two types of imagery were acquired at different seasons and local time in 2003, the Sun-target-sensor geometries are very different for these two scenes. As a result, shadows in the NAIP imagery are not shadowed in the QuickBird imagery and vice versa, which helps in discriminating land covers covered underneath.

In conclusion, accurate land-use information derived from high-resolution remote-sensing data combined with land-cover change analysis and GIS modelling can be used to estimate present environmental effects from land-use and land-cover changes. Through GIS modelling, it is also possible to evaluate site plans and model development scenarios in order to set planning priorities and to determine acceptable development or conservation practice. The spatiotemporal inventory of LULCC information and environmental impacts analysis from this study may provide important inputs for urban planning and environmental management. In the future, further analysis will be conducted by coupling urban growth model to predict future environmental change.

Acknowledgements

This study is funded by 2006 Faculty Research Grant of the Minnesota State University, Mankato. The support of the Department of Geography is gratefully acknowledged. Chris Kaczmarek helped in obtaining the historical air photographs and some aspects of the image preprocessing. The author also wants to thank all the reviewers and the editor for their constructive comments and suggestions.

References

ADAMS, J.S., KOEPP, J.A. and VANDRASEK, B.J., 2003, Urbanization of the Minnesota countryside: population change and low-density development near Minnesota's regional centers, 1970–2000. *Transportation and Regional Growth (TRG) Report No. 10*.

AMERICAN FORESTS, 2004, *User Manual, CITYgreen for ArcGIS* (Washington, DC: American Forests).

ANTROP, M., 2004, Landscape change and the urbanization process in Europe. *Landscape and Urban Planning*, **67**, pp. 9–26.

ARNOLD, C.L. and GIBBONS, C.J., 1996, Impervious surface coverage: the emergence of a key environmental indicator. *Journal of American Planning Association*, **62**, pp. 243–258.

ARTHUR, S.T., CARLSON, T.N. and CLARKE, K.C., 2003, Satellite and ground-based microclimate and hydrologic analyses coupled with a regional urban growth model. *Remote Sensing of Environment*, **86**, pp. 385–400.

BARALDI, A. and PARMIGGIANI, F., 1995, An investigation of the textural characteristics associated with gray level concurrence matrix statistical parameters. *IEEE Transactions on Geoscience and Remote Sensing*, **33**, pp. 293–304.

BAUER, M., LOEFFELHOLZ, B. and WILSON, B., 2005, Estimation, mapping and change analysis of impervious surface area by Landsat remote sensing. In *Proceedings, Pecora 16 Conference, American Society of Photogrammetry and Remote Sensing Annual Conference*, 23–27 October 2005, Sioux Falls, SD, CD-ROM.

CARLSON, T.N., 2004, Analysis and prediction of surface runoff in an urbanizing watershed using satellite imagery. *Journal of the American Water Resources Association*, **40**, pp. 1087–1098.

CARLSON, T.N. and ARTHUR, S.T., 2000, The impact of land use-land cover changes due to urbanization on surface microclimate and hydrology: a satellite perspective. *Global and Planetary Change*, **25**, pp. 49–65.

CLAGGETT, P.R., JANTZ, C.A., GOETZ, S.J. and BISLAND, C., 2004, Assessing development pressure in the Chesapeake Bay watershed: an evaluation of two land-use change models. *Environmental Monitoring and Assessment*, **94**, pp. 129–146.

COLLINGE, S.K., 1996, Ecological consequences of habitat fragmentation: implications for landscape architecture and planning. *Landscape Urban Planning*, **36**, pp. 59–77.

COPPIN, P.R. and BAUER, M.E., 1994, Processing of multitemporal Landsat TM imagery to optimize extraction of forest cover change features. *IEEE Transactions on Geoscience and Remote Sensing*, **32**, pp. 918–927.

DOUGHERTY, M., DYMOND, R.L., GOETZ, S.J., JANTZ, C.A. and GOULET, N., 2004, Evaluation of impervious surface estimates in a rapidly urbanizing watershed. *Photogrammetric Engineering and Remote Sensing*, **70**, pp. 1275–1284.

ELIASSON, I., 1992, Infrared thermography and urban temperature patterns. *International Journal of Remote Sensing*, **13**, pp. 869–879.

EURIMAGE, 2006, Products and Services Guide—QuickBird. Available online at: http://www.eurimage.com/products/docs/QuickBird.pdf (accessed 27 December 2006).

FOODY, G.M., 1999, The continuum of classification fuzziness in thematic mapping. *Photogrammetric Engineering and Remote Sensing*, **65**, pp. 443–451.

GILLIES, R.R., BOX, J.B., SYMANZIK, J. and RODEMAKER, E.J., 2003, Effects of urbanization on the aquatic fauna of the Line Creek watershed, Atlanta—a satellite perspective. *Remote Sensing of Environment*, **86**, pp. 411–422.

GONG, P. and HOWARTH, P.J., 1990, The use of structural information for improving land-cover classification accuracies at the rural–urban fringe. *Photogrammetric Engineering and Remote Sensing*, **56**, pp. 67–73.

HEROLD, M., LIU, X. and CLARKE, K.C., 2003, Spatial metrics and image texture for mapping urban land use. *Photogrammetric Engineering and Remote Sensing*, **69**, pp. 991–1001.

LEICA GEOSYSTEMS, 2005, *ERDAS IMAGINE Field Guides* (Atlanta, GA: GIS & Mapping, LLC).

MILESI, C., ELVIDGE, C.D., NEMANIA, R.R. and RUNNINGA, S.W., 2003, Assessing the impact of urban land development on net primary productivity in the southeastern United States. *Remote Sensing of Environment*, **86**, pp. 401–410.

NIKOLAKAKI, P., 2004, A GIS site-selection process for habitat creation: estimating connectivity of habitat patches. *Landscape and Urban Planning*, **68**, pp. 77–94.

OKE, T.R., 1976, City size and the urban heat island. *Atmospheric Environment*, **7**, pp. 769–779.

ODE, A. and FRY, G., 2006, A model for quantifying and predicting urban pressure on woodland. *Landscape and Urban Planning*, **77**, pp. 17–27.

POHL, C. and VAN GENDEREN, J.L., 1998, Multisensor image fusion in remote sensing: concepts, methods, and applications. *International Journal of Remote Sensing*, **19**, pp. 823–854.

REESE, H.M., LILLESAND, T.M., NAGEL, D.E., STEWART, J.S., GOLDMANN, R.A. SIMMONS, T.E., CHIPMAN, J.W. and TESSAR, P.A., 2002, Statewide land cover derived from multiseasonal Landsat TM data a retrospective of the WISCLAND project. *Remote Sensing of Environment*, **82**, pp. 224–237.

RIDD, M.K., 1995, Exploring the VIS model for urban ecosystems analysis through remote sensing. *International Journal of Remote Sensing*, **16**, pp. 2165–2186.

RYHERD, S. and WOODCOCK, C., 1996, Combining spectral and texture data in the segmentation of remotely sensed images. *Photogrammetric Engineering and Remote Sensing*, **62**, pp. 181–194.

SAWAYA, K.E., YUAN, F. and BAUER, M.E., 2001, Monitoring landscape change with Landsat classification. In *ASPRS Annual Conference*, 23–27 April 2001, St. Louis, MO, CD-ROM.

SCHUELER, T., 1994, The importance of imperviousness. *Watershed Prediction Technologies*, **3**, pp. 100–111.

SUTTON, P.G., 2003, A scale-adjusted measure of 'urban sprawl' using nighttime satellite imagery. *Remote Sensing of Environment*, **86**, pp. 353–369.

THOMAS, N., HENDRIX, C. and CONGALTON, R.G., 2003, A comparison of urban mapping methods using high-resolution digital imagery. *Photogrammetric Engineering and Remote Sensing*, **69**, pp. 963–972.

TILMAN, D., FARGIONE, J., WOLFF, B., D'ANTONIO, C., DOBSON, A., HOWARTH, R., SCHINDLER, D., SCHLESINGER, W.H., SIMBERLOFF, D. and SWACKHAMER, D., 2001, Forecasting agriculturally driven global environmental change. *Science*, **292**, pp. 281–284.

TONG, S.T.Y. and CHEN, W., 2002, Modelling the relationship between land use and surface water quality. *Journal of Environmental Management*, **66**, pp. 377–393.

UNITED STATES DEPARTMENT OF AGRICULTURE (USDA), NATURAL RESOURCES CONSERVATION SERVICE (NRCS), 1995, *State Soil Geographic (STATSGO) Data Base Data Use Information* (Washington, DC: USDA).

UNITED STATES DEPARTMENT OF AGRICULTURE (USDA), SOIL CONSERVATION SERVICE (SCS), 1985, *National Engineering Handbook. Section 4-Hydrology*, Chapters 4–10 (Washington, DC: USDA).

UNITED STATES DEPARTMENT OF AGRICULTURE (USDA), SOIL CONSERVATION SERVICE (SCS), 1986, *Urban Hydrology for Small Watersheds, Technical Release 55* (Washington, DC: USDA).

VISUAL LEARNING SYSTEMS, 2005, *Reference Manual, Feature Analyst 4.0 for Imagine* (Missoula, MT: Visual Learning Systems).

WENG, Q., 2001a, A remote sensing–GIS evaluation of urban expansion and its impact on surface temperature in the Zhujiang Delta, China. *International Journal of Remote Sensing*, **22**, pp. 1999–2014.

WENG, Q., 2001b, Modelling urban growth effects on surface runoff with the integration of remote sensing and GIS. *Environmental Management*, **28**, pp. 737–748.

WENG, Q. and YANG, S., 2006, Urban air pollution patterns, land use, and thermal landscape: an examination of the linkage using GIS. *Environmental Monitoring and Assessment*, **117**, pp. 463–489.

WOLTER, P.T., MLADENOFF, D.J., HOST, G.E. and CROW, T.R., 1995, Improved forest classification in the Northern Lake States using multi-temporal Landsat imagery. *Photogrammetric Engineering and Remote Sensing*, **61**, pp. 1129–1143.

YUAN, F. and BAUER, M.E., 2006, Mapping impervious surface area using high resolution imagery: a comparison of object-oriented classification to per-pixel classification. In *Proceedings, American Society of Photogrammetry and Remote Sensing Annual Conference*, 1–5 May 2006, Reno, NV, CD-ROM.

YUAN, F., SAWAYA, K.E., LOEFFELHOLZ, B.C. and BAUER, M.E., 2005, Land cover mapping and change analysis in the Twin Cities Metropolitan Area with Landsat remote sensing. *Remote Sensing of Environment*, **98**, pp. 317–328.

ZHANG, Y., 1999, Optimisation of building detection in satellite images by combining multispectral classification and texture filtering. *ISPRS Journal of Photogrammetry and Remote Sensing*, **54**, pp. 50–60.